Journal of Catalysis 241 (2006) 14-19

Growth and structural stability of well-ordered PdZn alloy nanoparticles

S. Penner[1*], B. Jenewein[1], H. Gabasch[1,2], B. Klötzer[1], D. Wang[2], A. Knop-Gericke[2], R. Schlögl[2], K. Hayek[1]

[1]Institute of Physical Chemistry, University of Innsbruck, Innrain 52a, A-6020 Innsbruck, Austria
[2]Department of Inorganic Chemistry, Fritz-Haber-Institute of the MPG, Faradayweg 4-6, 14195 Berlin, Germany

[*] Corresponding author: e-mail simon.penner@uibk.ac.at, phone +43 512 507 5056, fax +43 512 507 2925

Received: 16 february 2006, revised 3 April 2006, accepted 6 April 2006,available online 15 May 2006

Abstract

Despite many recent attempts to unravel the structure of novel PdZn alloys, promising catalysts in methanol steam reforming, a detailed study on the formation of Pd-Zn alloy particles and of their structural and thermal stability is still missing. We take advantage of the unique properties of epitaxially grown Pd particles embedded in layers of amorphous ZnO and mechanically stabilized by SiO_2, and present an electron microscopy study of the preparation of well-ordered PdZn alloy nanoparticles at surprisingly low reduction temperatures. They are formed by topotactic growth on the surface of the Pd nanoparticles and are structurally and thermally stable in a broad temperature regime (473 – 873 K). At and above 873K, partial decomposition of PdZn and beginning interaction with the SiO_2 support has been observed.

Keywords: Thin film model catalyst, hydrogen reduction, alloy formation, electron microscopy, selected area electron diffraction

Manuscript

Much recent effort has been invested in the development of suitable catalysts for methanol steam reforming[1-15] as this is one of the most promising processes for hydrogen production with a high hydrogen-to-carbon ratio[16]. Cu/ZnO catalysts have been commercially used to produce hydrogen with high selectivity and activity[2-6], but they suffer from deactivation at reaction temperatures above 573 K[17]. Recently, novel Pd/ZnO systems[3-15] (as well as Pd/Ga_2O_3 and Pd/In_2O_3[18,19]) have attracted more attention because of their enhanced long-term and thermal stability[20,21]. As unsupported pure Pd exhibits only a poor selectivity[22], the observed high activity and selectivity for CO_2 formation was ascribed to the formation of distinct PdZn, PdIn and PdGa alloys upon reductive activation at elevated temperatures[18]. Best characterized is the Pd/ZnO system, where alloy formation has been studied and confirmed by X-ray diffraction (XRD)[18,23], temperature-programmed reduction (TPR)[18,23] and X-ray and ultraviolet photoelectron spectroscopy (XPS and UPS)[24-26]. Iwasa et al.[23] observed PdZn alloy formation upon reduction at very low T (≥ 473 K). Density functional studies revealed the close relationship between the electronic structure of PdZn and Cu-based catalysts giving rise to a similar catalytic performance in methanol steam reforming[27,28]. Comparatively few studies have been carried out on the structural characterization of the PdZn alloys by electron microscopy, and these were limited to overview imaging of powder catalysts in the as-prepared state and after hydrogen reduction, thereby mainly supporting XRD measurements[29,30]. The Pd-Zn system is known to form several stable bulk alloy phases[31]. The most important and thermally most stable is the PdZn (β1) phase, which crystallizes in a tetragonal (AuCu-type) $L1_0$ structure[32]. A key point for understanding the catalytic pecularities of the above-mentioned Pd-Zn alloy particles is also to determine their surface composition. Recent experiments in our laboratory[33] show that a well-ordered (6x4/√3) Pd-Zn layer forms on Pd(111) under UHV conditions at elevated temperature.

Despite the importance of PdZn alloys for hydrogen production by steam reforming, detailed transmission electron microscopy (TEM) studies of their morphology and structure are not yet available. The aim of this study is therefore to exploit the capabilities of modern electron microscopes to resolve the atomic structure of catalysts and to start from well defined Pd particles, epitaxially grown on NaCl(001) cleavage faces and subsequently embedded in a layer of ZnO, to prepare distinct PdZn alloys. We shall be able to present the first high-resolution images of well-defined PdZn alloy particles and to propose a mechanism of their formation, as well as detailed information on their thermal and structural stability.

Pd metal was deposited by electron-beam evaporation onto a freshly-cleaved NaCl(001) plane at a base pressure of 10^{-4} Pa and a substrate temperature of 623 K. Under these experimental conditions, the deposition of Pd films of about 0.5nm nominal thickness results in well-shaped Pd particles about 5 nm in size. Subsequently, the Pd particles were covered by a layer of amorphous ZnO at 523K template temperature and mechanically stabilized by a supporting layer of amorphous SiO_2 (nominal thickness: 25nm), deposited at room temperature. NaCl was subsequently removed by dissolution in distilled water and after careful rinsing the resulting thin films were dried and mounted on gold grids for electron microscopy. Reductive treatments (1 bar H_2 for 1h) were performed in parallel in a flow system and a circulating batch reactor in the temperature range between 473 and 873 K. Structural and morphological changes were followed by (high-resolution) electron microscopy (HRTEM), selected area electron diffraction (SAED) and energy-dispersive X-ray spectroscopy (EDXS). The electron micrographs were taken with a ZEISS EM 10C, and with a CM FEG microscope equipped with a Gatan image filter GIF100.

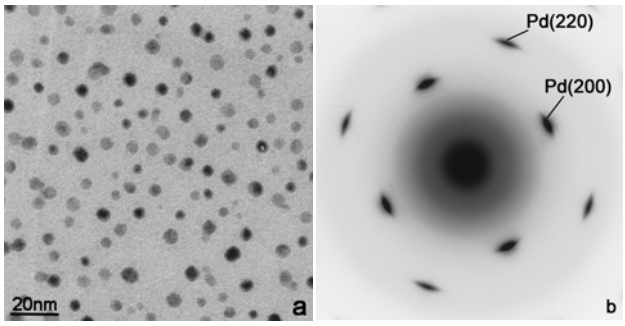

Figure 1: (a) TEM overview of as-deposited Pd particles and ZnO/SiO_2 support, (b) corresponding SAED pattern.

The TEM overview in Fig. 1a shows the as-deposited state of the Pd catalyst, to which we reference all structural alterations occurring upon reductive activation. The Pd particles are visible as dark and grey dots with a mean diameter of ~ 5nm. A particle density of around $6.8x10^7$ particles/cm^2 was estimated by evaluating a number of TEM images from different parts of the sample. The dark particles are perfectly aligned along the Bragg orientation, the grey ones slightly tilted out of the respective Bragg position. Most particles exhibit square or rectangular shapes, whereas some have more rounded outlines. Weak-beam dark field images of the corresponding alumina-based Pd thin film catalysts revealed the cuboctahedral habit of these particles[34]. Their almost perfect relative orientation with respect to the former NaCl(001) single crystal substrate is confirmed by the SAED pattern (Fig. 1b), exhibiting exclusively reflections of the fcc structure of the Pd particles oriented along the [001] zone axis, i.e. Pd(200) and Pd(220) spots. No reflections arising from other orientations are present. HRTEM images (Fig. 2) of cuboctahedral particles mainly show (200) lattice fringes of fcc Pd [d_{200}(Pd)=0.1945nm], including an angle of 45° with the (111) cuboctaeder faces[34]. Hence, most Pd particles exhibit (001) base planes perpendicular to the electron beam. Both the ZnO and the SiO_2 support are amorphous in the as-grown state. The amount of deposited ZnO was verified by EDXS to be close to the amount of deposited Pd.

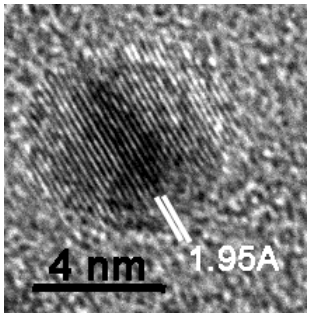

Figure 2: HRTEM image of an as-grown Pd particle exhibiting (200) lattice fringes.

No significant changes in particle structure or morphology were noticed upon reduction at temperatures below 473 K (1 bar hydrogen for 1h). However, considerable alterations in both the morphology and composition are introduced if the reduction temperature is raised to 523 K (Fig. 3). The particle size is slightly increased compared to the as-deposited state (5.3 nm mean diameter, particle density: $5.6x10^7$ particles/cm^2), and recrystallization has occurred. A major part of the particles show randomly arranged sharp edges (denoted "A" in Fig. 3a), while square and rectangular particles with sharp outlines are also present (denoted "B" in Fig. 3a). This morphology is in striking contrast to both the as-grown state of this catalyst (Fig. 1a) and the state of a Pd/SiO_2 reference catalyst without ZnO, but treated under otherwise identical conditions (1 bar H_2 for 1h at 523 K, see Figs. 3c and d), which is discussed below. SAED patterns (Fig. 3b) and high-resolution images (Fig. 4) confirm the observed morphology changes. The SAED patterns of Fig. 3b show a "doubling" of both the Pd (200) and the Pd (220) spots, i.e. new reflections arise at d ~ 0.144 nm and d ~ 0.205 nm, and four new spot reflections appear at ~ 0.291 nm, rotated by 45° with respect to the Pd (200) spots. These new reflections perfectly

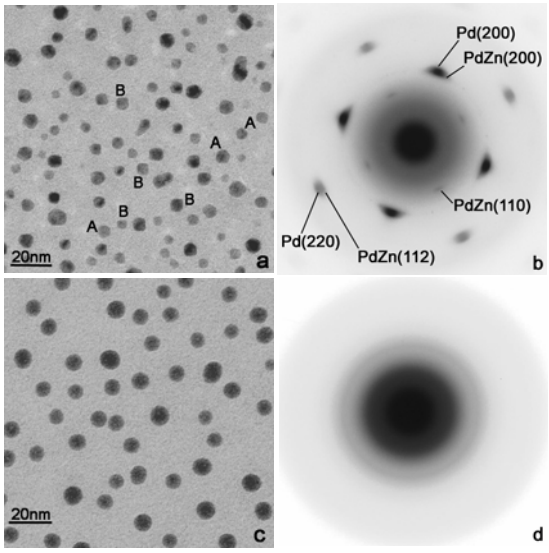

Figure 3: (a) TEM overview of the $Pd/ZnO/SiO_2$ catalyst after reduction in 1 bar hydrogen at 523 K for 1 h, (b) corresponding SAED pattern; (c) TEM overview of the Pd/SiO_2 reference catalyst after reduction in 1 bar hydrogen at 523 K for 1 h, (d) corresponding SAED pattern.

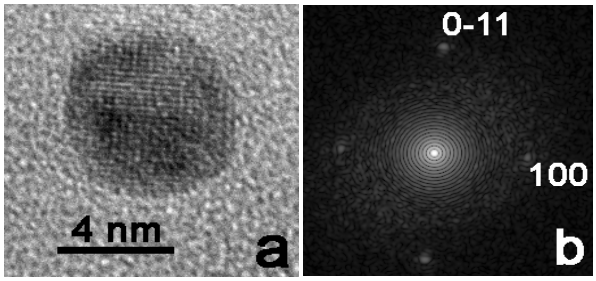

Figure 4: (a) HRTEM image of a single-crystalline PdZn particle on its [011] zone axis, (b) corresponding FFT.

match the (112), (200) and (110) reflections of the tetragonal PdZn alloy phase ($L1_0$ AuCu-type structure)[32] (d_{112}(PdZn) = 0.1449 nm, d_{200}(PdZn) = 0.205 nm, d_{110}(PdZn) = 0.290 nm), which was formed to some extent during reductive activation even at 473 K. We emphasize that this newly formed alloy phase grows in almost perfect crystallographic relationship to the underlying Pd lattice (Pd [100] // PdZn [100]). This result is further corroborated by parallel high-resolution imaging. Fig. 4 shows a single PdZn alloy particle along with its fast Fourier transform (FFT). According to the FFT, the lattice fringes can be addressed to the (100) and (0-11) distances of the tetragonal PdZn crystal structure[32]. Hence, the particle is oriented along its [011] zone axis. Similar effects have already been observed on the corresponding Pt/SiO_2[35] and Pt/CeO_2[36] systems. On the Pd/SiO_2 reference catalyst without ZnO, which was reduced under otherwise identical conditions, the introduction of higher-indexed facets, manifested as a rounding of particles in TEM[34] and a considerable increase of particle size due to coalescence was observed (Fig. 3c), which is in strong contrast to the effects observed on $Pd/ZnO/SiO_2$ (Fig. 3a). Compared to the $Pd/ZnO/SiO_2$ catalyst, the SAED patterns of Pd/SiO_2 catalysts after reduction at 523 K (Fig. 3b) clearly reflect a trend towards amorphous structures, which may be interpreted in terms of Pd hydride formation[37]. From the comparison of Figs. 3a and b on the one hand and Figs 3c and d on the other hand, it is obvious that the above-discussed recrystallization of the Pd particles in contact with ZnO must be closely associated to the process of alloy formation. Thus, adding ZnO to the Pd/SiO_2 system (i) structurally stabilizes the Pd particles by Pd-Zn alloy formation compared to Pd/SiO_2 and (ii) prevents the formation of an amorphous hydride phase. Furthermore, from this protection against hydride formation by the presence of ZnO one can deduce that already at low reduction temperatures the particles are covered by a shell of well-ordered PdZn alloy. This growth mechanism is confirmed by the fact that at $T \leq 523$ K metallic Pd is still present and by the perfect epitaxial relationship between Pd and PdZn. Most likely, a metastable PdZn alloy skin is formed *before* alloying proceeds into deeper regions of the Pd particles. Fig. 4 shows a HR image of a single PdZn alloy particle in the state of complete transformation already after reduction at 523 K. Since the SAED pattern shows metallic Pd remaining on the catalyst, complete PdZn particles as shown in Fig. 4 are still the minority species after 523 K reduction.

This "partially alloyed" state of the catalyst is stable up to 523 K. After reduction above 600 K, the Pd reflections vanish and only alloy-induced diffraction spots remain. TEM images taken after reduction at 723 K (Fig. 5a) reveal that the particle size has again slightly increased (mean diameter 5.5 nm, particle density: 5.2×10^7 particles/cm^2), confirming the high thermal stability of the PdZn alloy in comparison to the as-grown state and the state after reduction at 523 K. SAED patterns (Fig. 5b) show broadened PdZn reflections indicating a slight azimuthal disorder of the alloy particles. However, as no higher-order reflections of the tetragonal alloy structure are visible, it is clear that no additional particle zone axes contribute to the diffraction pattern. This underlines the high structural stability of the completed Pd-Zn alloy particles.

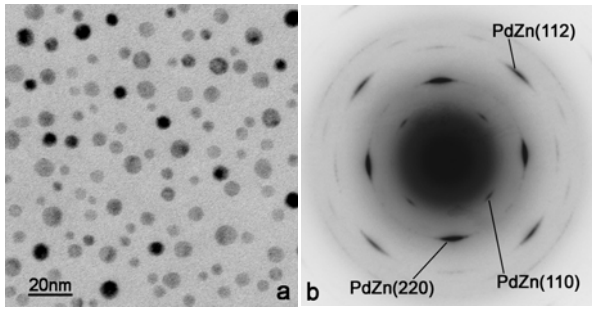

Figure 5: (a) TEM overview of the $Pd/ZnO/SiO_2$ thin film catalyst after reduction in 1 bar hydrogen at 723 K for 1h, (b) corresponding SAED pattern.

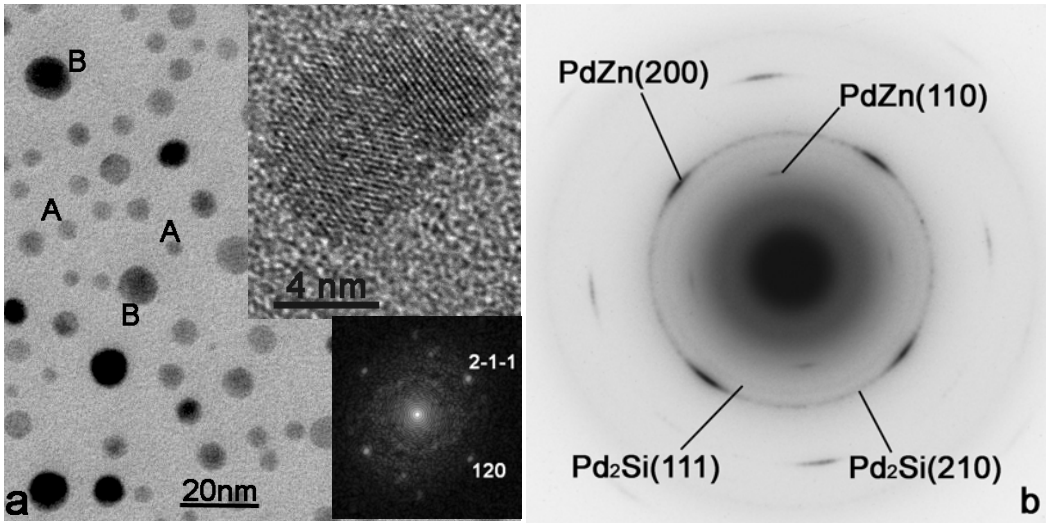

Figure 6: State of the $Pd/ZnO/SiO_2$ catalyst after reduction in 1 bar H_2 at 873 K for 1h. (a) TEM overview, (b) SAED pattern. Inset: HRTEM image of a [2,-1,-5] oriented Pd_2Si particle with its FFT.

By reduction at and above 873 K (Figs. 6a and b), again some structural alterations are observed. The majority of particles did not undergo coalescence but appear thermally and structurally stable even at ≥ 873 K (denoted "A" in Fig. 6a). Nevertheless, some considerably larger particles (denoted "B" in Fig. 6a) were formed, obviously by consuming closely neighboured particles. It is worth to notice that the sharp-angled particles have almost completely vanished and most particles now exhibit more rounded outlines. Increasing disorder is also evidenced by the SAED patterns in Fig. 6b. The PdZn (110) and (200) spots appear broadened and faint, pointing to an increasing loss of orientational order and/or partial decomposition of the PdZn alloy. In addition, the formation of a Pd_2Si alloy phase is documented by the SAED pattern (Fig. 6b) and by high-resolution imaging (inset in Fig. 6a), indicating that at about 900 K the stability limit of the $Pd/ZnO/SiO_2$ catalyst is reached. Weak Pd_2Si (111) and (210) reflections, the latter overlapping with the broadened PdZn(200) spots, appear in the electron diffraction patterns. The HRTEM image of a single Pd_2Si alloy particle (along with its FFT) as shown in the inset of Fig. 6a indicates that the particle is oriented along its [2-1-5] zone axis. The state of the catalyst after reduction at 873 K can therefore be characterized as a coexistence of PdZn and Pd_2Si alloy phases.

In line with previous studies on PdZn formation[8,12-14], the present electron microscopy study unambiguously reveals the onset of the formation of a tetragonal PdZn phase upon reduction at T ≥ 473 K. The formation of the alloy phase proceeds most likely via topotactic formation of PdZn on top of the Pd particles. This growth mechanism is probably favoured by the relatively small mismatch of the lattice constants of fcc Pd (0.388 nm) and tetragonal PdZn (0.410 nm). We emphasize that the properties of the special thin film model catalysts used for in present study favour the alloying kinetics. Compared to conventional impregnated catalysts the thin film systems are known for large and intimate contact between metal and support and defined particle size and shape (which makes them well-suited for plan view lattice imaging by HRTEM).

The main conclusions from this work are therefore: PdZn alloy particles are thermally and structurally stable upon reduction between 473 and 873 K. Even above 873 K only partial decomposition of the PdZn alloy was observed, accompanied by strong interaction with the SiO_2 support and resulting in the formation of Pd-rich silicides. This broad stability range is clearly due to the strong interaction of Pd with the ZnO support and the high stability of the 1:1 PdZn alloy phase. The strong particle stabilization effect (SPSE) is of importance for catalytic processes such as methanol steam reforming and methanol synthesis on Pd/ZnO catalysts. In particular, the striking differences between the Pd/SiO_2 and $Pd/ZnO/SiO_2$ systems demonstrated in this work may lead to a better understanding of the drastic activity and selectivity differences between Pd/SiO_2 and Pd/ZnO reported in the literature[13,23]. According to recent single crystal experiments[33,38] and theory studies[38,39] it seems that this very stable PdZn alloy phase of stoichiometric surface composition is stable over a wide range of temperatures.

Acknowledgement

H. G. thanks the Max-Planck-Society for a FHI research grant

References

[1] H. Kobayashi, N. Takezawa, C. Minochi, J. Catal. 69 (1981) 487.
[2] T.-J. Huang, S.-W. Wang, Appl. Catal. 24 (1986) 287.
[3] T.-J. Huang, S.-L. Chren, Appl. Catal. 40 (1988) 43.
[4] S. Velu, K. Suzuki, M.P. Kapoor, F. Ohashi, T. Osaki,met Appl. Catal. A 213 (2001) 47.
[5] S. Velu, K. Suzuki, M. Okazaki, M.P. Kapoor, T. Osaki, F. Ohashi, J. Catal. 194 (2000) 373.
[6] S. Murcia-Mascaro´ s, R.M. Navarro, L. Gomez-Sainero,U. Costantino, M. Nocchetti,,L.G. Fierro, J. Catal. 198 (2001) 338.
[7] N. Takezawa, N. Iwasa, Catal. Today 36 (1997) 45.
[8] N. Iwasa, S. Masuda, N. Ogawa, N. Takezawa, Appl. Catal. A 125 (1995) 145.
[9] M.L. Cubeiro, J.L.G. Fierro, J. Catal. 179 (1998) 150.
[10] M.L. Cubeiro, J.L.G. Fierro, Appl. Catal. A 168 (1998) 307.
[11] Y.-H. Chin, R. Dagle, J. Hu, A.C. Dohnalkova, Y. Wang, Catal. Today 77 (2002) 79.
[12] N. Iwasa, T. Mayanagi, S. Masuda, N. Takezawa, React. Kinet. Catal. Lett. 69 (2000) 355.
[13] N. Iwasa, T. Mayanagi, W. Nomura, M. Arai, N. Takezawa, Appl. Catal. A 248 (2003)153.
[14] N. Iwasa, W. Nomura, T. Mayanagi, S. Fujita, M. Arai, N. Takezawa, J. Chem. Eng. Jpn.37 (2004) 286.
[15] Y. Suwa, S.-I. Ito, S. Kameoka, K. Tomishige, K. Kunimori, Appl. Catal. A 267 (2004) 9.
[16] R. Peters, H.G. Dunsterwald, B. Hohlein, J. Power Sources 86 (2000) 507.
[17] D.L. Trimm, Z. I. Önsan, Catal Rev. 43 (2001) 31.
[18] N. Iwasa, N. Takezawa, Top. Catal. Vol.22 3-4 (2003) 215.
[19] N. Iwasa, S. Masuda, N. Ogawa, N. Takezawa, Appl. Catal. A 125 (1995) 145.
[20] S. Liu, K. Takahashi, M. Ayabe, Catal. Today 87 (2003) 247.
[21] S. Liu, K. Takahashi, K. Uematsu, M. Ayabe, Appl. Catal. A 277 (2004) 265.
[22] N. Takezawa, N. Iwasa, Catal. Today 36 (1997) 45.
[23] N. Iwasa, T. Mayanagi, N. Ogawa, K. Sakata and N. Takezawa, Catal. Lett. 54 (1998) 119.
[24] A. Bayer, K. Flechtner, R. Denecke, H.-P. Steinrück, K.M. Neyman, N. Rösch, Surf. Sci. 600 (2006) 78.
[25] N. Iwasa, N. Ogawa, S. Masuda, N. Takezawa, Bull. Chem. Soc. Jpn. 71 (1998) 1451.
[26] S. Liu, K. Takahashi, K. Fuchigami, K. Uematsu, Appl.Catal. A 299 (2006) 58.
[27] Z.-X. Chen, K.M. Neyman, A.B. Gordienko, N. Rösch, Phys. Rev. B 68 (2003) 75417.
[28] Z.-X. Chen, K.M. Neyman, N. Rösch, Surf. Sci. 548 (2004) 291.
[29] J. Agrell, G. Germani, S.G. Järas, M. Boutonnet, Appl. Catal. A, 242 (2003) 233.
[30] Y. Suwa, S. Ito, S. Kameoka, K. Tomishige, K. Kunimori, Appl. Catal. A 267 (2004) 9.
[31] Landolt-Börnstein Vol.5 Phase Equilibria, Crystallographic and Thermodynamic Data of Binary Alloys, Springer, Berlin 1998.
[32] H. Nowotny, H. Bitter, Monatsh. Chemie 81 (1950) 679.
[33] H. Gabasch, S. Penner, B. Jenewein, B. Klötzer, A. Knop-Gericke, D. Wang, R. Schlögl, K. Hayek, Surface Science, *submitted.*
[34] G. Rupprechter, K. Hayek, L. Rendon, J.M. Yacaman, Thin Solid Films 260 (1995) 148.
[35] D. Wang, S. Penner, D.S. Su, G. Rupprechter, K. Hayek, R. Schlögl, J. Catal. 219 (2003) 434.
[36] S. Penner, D. Wang, R. Podloucky, R. Schlögl, K. Hayek, PhysChemChemPhys 6 (2004) 5244.
[37] S. Penner, B. Jenewein, H. Gabasch, B. Klötzer, D. Wang, A. Knop-Gericke, R. Schlögl, K.Hayek, *unpublished work.*
[38] A. Bayer, K. Flechtner, R. Denecke, H.-P. Steinrück, K. N. Neyman, N. Rösch, Surf. Sci. 600 (2006) 78.
[39] Z. Chen, K. N. Neyman, N. Rösch, Surf. Sci. 548 (2004) 291.